**June 11, 2013**

# OBSERVATIONS CONCERNING VORTEX-INDUCED VIBRATIONS

**by Paul Paslay, P. E. #44278**

## INTRODUCTION

This study "returns" to an important case of vortex-induced vibrations (VIV) that has been studied for over 60 years. Den Hartog[1] has described the phenomenon and cited several occurrences of practical importance. A review of VIV studies up to 1994 is provided by Blevins[2] in his comprehensive treatise. The progress made in understanding the phenomena and documentation of specific cases is significant. A commercial computer program[3] is available for offshore marine risers.

An elementary analysis useful for design is presented using observations cited in earlier work[2]. The case for a straight, uniform, beam-column simply supported at each end and subjected to a uniform velocity fluid flow perpendicular to the beam-column axis is considered. The axial effective force on the beam-column is constant and its cross section is for a standard circular tube. The fluid surrounding the beam-column is infinite in extent. Elementary, conventional equations and assumptions are used in the analysis of this case. The case of most interest (resonance case) is when the frequency of oscillation of the vortex forces equals the fundamental natural frequency of the beam column. The resonance case mode shape is a half sine wave. The resonance case is the only one considered in this work. The results of the analysis predict the motions both perpendicular and parallel to the flow direction. Since all of the required initial conditions are not known a priori, the numerical integration of the equations is extended to 10 cycles which is adequate for determining the steady-state prediction.

The steady-state predictions obtained from the analysis may be more useful for some problems than one may initially recognize. For example, marine risers are usually sufficiently long so that the vortex exciting frequency from ocean currents is many times (typically 30 to 50 times) the fundamental natural frequency of the riser. The higher natural frequency mode shapes resemble sine waves so that each half wave in the riser mode shape may be approximated as a single, simply supported beam-column under constant tension. Furthermore, for the higher modes the end conditions for the riser ends have little influence, except near the top and bottom of the riser, on the mode shapes and natural frequencies of the riser. Another way of modeling such a problem is that every vortex exciting frequency is a natural frequency. This view is further supported by the experimental observation that the vortex exciting frequencies will shift a bit so they can be synchronous with the riser natural frequency. Since the tension varies with depth in a riser several predictions from the analysis presented here should be sufficient to establish the expected stress and displacement amplitude levels in the riser and the necessity for adding vibration suppressors to the riser (see Reference 2, Section 3.6).

**NOMENCLATURE**

$C_D$ = constant drag coefficient for beam-column
$C_L$ = constant lift coefficient caused by vortex shedding
$D$ = uniform diameter of beam-column
$\tilde{E} = EI \cdot \left(\frac{\pi}{L}\right)^4 + TE \cdot \left(\frac{\pi}{L}\right)^2$
$EI$ = uniform bending stiffness of beam-column
$F_D$ = drag force/length on beam-column, a function of t and x
$F_L$ = lift force/length on beam-column, a function of t and x
$F_X$ = x-component of force/length on beam-column, a function of t and x
$F_Y$ = y-component of force/length on beam-column, a function of t and x
$L$ = length of beam-column between adjacent, simple supports
$m$ = uniform mass/length for beam-column
$\tilde{m}$ = uniform added mass/length from fluid
$S$ = Strouhal number
$TE$ = constant effective tension in beam-column
$t$ = time, an independent variable
$U$ = uniform flow velocity in the negative z direction, perpendicular to the rod axis
$V$ = relative velocity magnitude of flow to strumming beam-column
$Y = \frac{\omega \cdot \bar{y}}{U}$
$y$ = coordinate to center of beam-column and lateral to flow, a function of t and x
$\bar{y}$ = value of y at center of beam-column, a function of t
$Z = \frac{\omega \cdot \hat{z}}{U}$
$z$ = parallel to flow coordinate to center of beam-column, a function of t and x
$\bar{z}$ = value of z at center of beam-column, a function of t
$\hat{z} = \bar{z} + \frac{\pi}{4} \cdot \frac{\rho \cdot D \cdot C_D \cdot U^2}{EI \cdot \frac{\pi^4}{L^4} + TE \cdot \frac{\pi^2}{L^2}}$
$\dot{\alpha} \equiv \frac{\partial \alpha}{\partial t}$
$\beta$ = inclination of V to flow direction
$\zeta$ = uniform structural damping parameter for beam-column
$\mu$ = absolute viscosity of flowing fluid
$\nu$ = kinematic viscosity of flowing fluid
$\rho$ = mass density of flowing fluid
$\omega$ = circular frequency for $F_L$
$\omega_n$ = fundamental, natural, circular frequency of submerged beam-column

## REVIEW OF ELEMENTARY EQUATIONS AND ENSUING MANIPULATIONS

### A. STROUHAL NUMBER

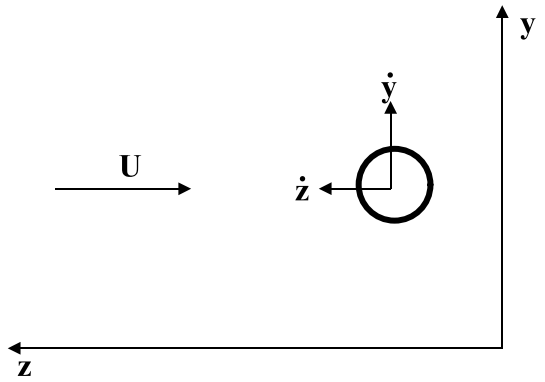


The above sketch shows a generic cross section of a rod whose axis, the x-axis, is perpendicular to the page. The rod is simply supported at each end and subjected to a uniform velocity of magnitude U in the negative z direction. The absolute velocities, $\dot{y}$ and $\dot{z}$, in the y and z directions are shown in the sketch.

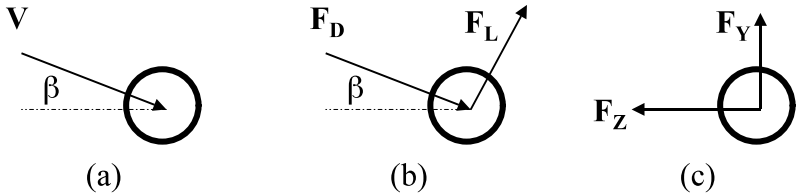


The sketch immediately above shows a) the relative fluid velocity vector, V, with respect to the rod at its inclination, β, to the z-axis, b) the resulting drag and lift forces $F_D$ and $F_L$ and c) the resolution of $F_D$ and $F_L$ into $F_Y$ and $F_Z$ in the y and z directions. Recall that, in practical cases, the maximum, single-peak amplitude of lateral motion, $y_{max}$, is roughly equal to the riser outer diameter, D. Therefore the maximum lateral velocity is, approximately, the product of $y_{max}$ and the circular strumming frequency, ω, as deduced by the Strouhal number[4]. The ratio of this maximum lateral velocity to the free stream velocity, U, is,

$$\frac{(\text{maximum lateral velocity})}{(\text{free stream velocity})} \cong \frac{\omega \cdot y_{max}}{U}$$

Under typical circumstances the Strouhal number, S, is approximately equal to 0.2 and it is defined by,

$$S = \frac{\omega \cdot D}{2 \cdot \pi \cdot U}$$

so that,

$$\frac{(\text{max imum lateral velocity})}{(\text{free stream velocity})} = \frac{2 \cdot \pi \cdot S \cdot y_{max}}{D} \cong 1.257 \cdot \frac{y_{max}}{D}$$

In addition, the experimentally observed value of $y_{max}$ is usually equal, approximately, to D so that the above velocity ratio is equal, approximately, to one. Consequently, the maximum value of the angle β shown in the second sketch above is too large to be treated as a linearized perturbation.

Careful measurements of the vortex exciting frequency have shown that the Strouhal number is a function of Reynolds' number; see Reference 2, page 48, Figure 3.3. The Reynolds' number, RE, is defined as,

$$RE = \frac{\rho \cdot V \cdot D}{\mu}$$

For the numerical scheme in this analysis, values of S = S(RE) from the figure below are used.

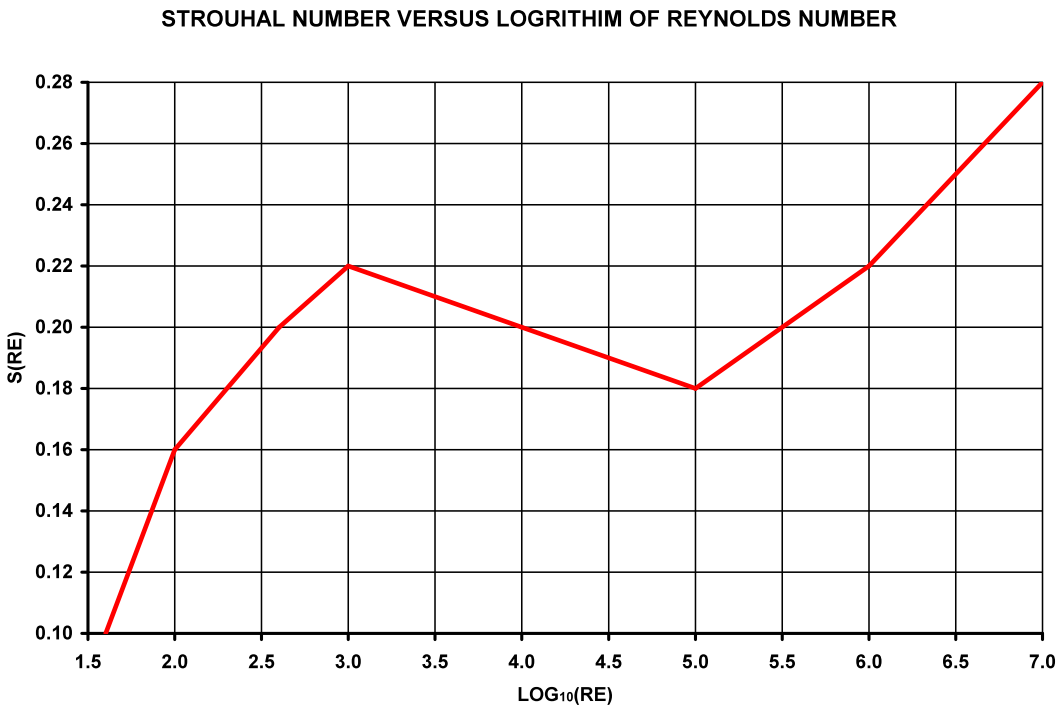

## B. DRAG AND LIFT FORCES

Since β cannot be modeled as being small compared to one, the following expressions are appropriate,

$$V = \sqrt{(U + \dot{z})^2 + \dot{y}^2} \quad > 0$$

$$\sin\beta = \frac{\dot{y}}{\sqrt{(U + \dot{z})^2 + \dot{y}^2}}$$

$$\cos\beta = \frac{(U + \dot{z})}{\sqrt{(U + \dot{z})^2 + \dot{y}^2}}$$

so that,

$$F_Y = -F_D \cdot \sin\beta + F_L \cdot \cos\beta$$

$$F_Z = -F_D \cdot \cos\beta - F_L \cdot \sin\beta$$

The values for $F_D$ and $F_L$ are not well established for cases where β varies rapidly with time. It is common in such situations to neglect the influence of the rapid β variation on the lift and drag forces so that the steady-state form of the lift and drag equations is used. This analysis also neglects the dynamic β influence on the lift and drag forces so that,

$F_L$ = classical lift force/length, $\rho \perp \mathbf{V} = \frac{1}{2} \cdot D \cdot C \cdot | \quad | \cdot \quad \cdot \quad _L \cdot \sin(\quad t \cdot \quad )$

$F_D$ = classical drag force / length, $\rho \| \mathbf{V} = \frac{1}{2} \cdot D \cdot C \cdot | \quad | \cdot \quad \cdot \quad _D$

so the equations for $F_Y$ and $F_Z$ become,

$$F_Y = \tfrac{1}{2} \cdot \rho \cdot V \cdot D \cdot (-C_D \cdot \dot{y} + C_L \cdot (U + \dot{z}) \cdot \sin(\omega \cdot t))$$

$$F_Z = -\tfrac{1}{2} \cdot \rho \cdot V \cdot D \cdot (C_D \cdot (U + \dot{z}) + C_L \cdot \dot{y} \cdot \sin(\omega \cdot t))$$

## C. ADDED MASS

When the beam-column moves relative to the fluid, the fluid in its vicinity also moves. The forces on the beam-column caused by the mass of the moving fluid must be taken into account if the lateral relative velocity changes. The phenomenon is represented as a mass added to the beam-column mass. The amount of this added mass is computed using a potential flow solution[2, 5]. Since the origin of the vortex force excitation is caused by a stagnation region oscillating on the beam-column surface, it is clear that the flow has a turbulent region in contradiction to the laminar flow implied by the potential flow solution. In spite of this shortcoming, the potential flow solution is normally used in other analyses and it will be used here. The added mass per unit length for the potential flow solution equals the mass per unit length of the displaced fluid, $\frac{1}{4}\cdot\rho\cdot\pi\cdot D^2$ and this value is used here and denoted by $\tilde{m}$.

## D. BEAM-COLUMN FUNDAMENTAL NATURAL FREQUENCY

The equations for beam-column theory[6] are a modification of the usual beam theory that includes the influences of an axial force applied to the beam. The equations are used extensively to obtain axial, compressive buckling loads. This study is restricted to axial tensile loads TE. The classical method for finding natural frequencies for beam-columns neglects all external forces except rigid support forces as well as damping forces. In this case the governing equation for motions in the x-y plane becomes (for the x-z plane replace y by z),

$$\left(m + \tilde{m}\right)\cdot \ddot{y} + EI\cdot y'''' - TE\cdot y'' = 0$$

where y = y(x,t), an overhead dot implies differentiation with respect to time, t, and the apostrophe symbol implies differentiation with respect to distance, x. The boundary conditions for this problem are,

$$y\left(0,t\right) = y\left(L,t\right) = y''\left(0,t\right) = y''\left(L,t\right) = 0$$

That is, the lateral displacements and moments vanish at x = 0 and x = L.

The x dependence for the fundamental mode shape for the above equations is removed with the following half sine wave expression,

$$y = y\left(x,t\right) = \bar{y}\left(t\right)\cdot \sin\left(\pi\cdot\frac{x}{L}\right) \equiv \bar{y}\cdot\sin\left(\pi\cdot\frac{x}{L}\right)$$

so that $\bar{y}$ is the single peak lateral amplitude of vibration at $x = \frac{1}{2}\cdot L$. When this expression is substituted into the above differential equation, the following equation results,

$$\ddot{\bar{y}} + \frac{EI\cdot\left(\frac{\pi}{L}\right)^4 + TE\cdot\left(\frac{\pi}{L}\right)^2}{m + \tilde{m}}\cdot\bar{y} = 0$$

Consequently, the beam-column fundamental natural frequency, $\omega_n$, is,

$$\omega_n = \sqrt{\frac{EI\cdot\left(\frac{\pi}{L}\right)^4 + TE\cdot\left(\frac{\pi}{L}\right)^2}{m + \tilde{m}}}$$

## E. DEVELOPMENT OF GOVERNING EQUATIONS

In Section D above the version of the governing beam-column equation for finding the natural frequency was given. When the external fluid forces and beam-column damping are included in those equations, the following equations result,

$$(m+\tilde{m})\cdot\ddot{y}+\xi_{2y}\cdot\omega_y\cdot\dot{y}\cdot EI\cdot y''''-TE\cdot y''=F_Y$$

$$(m+\tilde{m})\cdot\ddot{z}+\xi_{2z}\cdot\omega_z\cdot\dot{z}\cdot EI\cdot z''''-TE\cdot z''=F_Z$$

Inclusion of $F_Y$ and $F_Z$ in the equations causes them to be coupled. The equations given in Section B are now used to express $F_Y$ and $F_Z$ in terms of $C_D$, $C_L$, D, U, $\dot{y}$ and $\dot{z}$. The expression for V is expanded through second order terms in $\dot{y}$ and $\dot{z}$ to obtain.

$$V\cong U\cdot\left(1+\frac{\dot{z}}{U}+\frac{1}{2}\cdot\left(\frac{\dot{y}}{U}\right)^2\right)$$

When the equations,

$$y=y(x,t)=\bar{y}(t)\cdot\sin\left(\pi\cdot\frac{x}{L}\right)\equiv\bar{y}\cdot\sin\left(\pi\cdot\frac{x}{L}\right)$$

$$z=z(x,t)=\bar{z}(t)\cdot\sin\left(\pi\cdot\frac{x}{L}\right)\equiv\bar{z}\cdot\sin\left(\pi\cdot\frac{x}{L}\right)$$

are introduced, there is an explicit dependence of x in the equations. This dependence is artificially removed by integrating the equations on x from x = 0 to x = L and setting the results to zero. This approximation has an averaging influence on the equations. After these steps the first two equations of this section become,

$$(m+\tilde{m})\cdot\ddot{\bar{y}}+\xi_{2y}\cdot\omega_y\cdot\dot{\bar{y}}\cdot EI\cdot\bar{y}\cdot\left(\frac{\pi^4}{L^4}\right)+TE\cdot\bar{y}\cdot\frac{\pi^2}{L^2}$$
$$=\frac{\pi\cdot\rho\cdot D}{4\cdot U}\cdot\left[\begin{array}{l}C_L\cdot U^3\cdot\omega\cdot\sin(\omega\cdot t)-\frac{2}{\pi}\cdot U^2\cdot C_D\cdot\bar{y}+\frac{4}{\pi}\cdot U\cdot C_L\cdot\dot{\bar{z}}\cdot\sin(\omega\cdot t)-\frac{1}{2}\cdot U\cdot C_D\cdot\dot{\bar{y}}\cdot\bar{z}\cdot\dot{\bar{y}}\\+\frac{1}{2}\cdot C_L\cdot U\cdot\left(\dot{\bar{z}}^2+\frac{1}{\pi^2}\cdot\dot{\bar{y}}^2\right)\cdot\sin(\omega\cdot t)-\frac{4}{3\cdot\pi}\cdot C_D\cdot\bar{z}\cdot\dot{\bar{y}}^2\cdot\sin(\omega\cdot t)^2\cdot\dot{\bar{y}}-\frac{2}{3}\cdot C_L\cdot\dot{\bar{z}}^3\cdot\sin(\omega\cdot t)^3\end{array}\right]$$

$$(m+\tilde{m})\cdot\ddot{\bar{z}}+\xi_{2z}\cdot\omega_z\cdot\dot{\bar{z}}\cdot EI\cdot\bar{z}\cdot\left(\frac{\pi^4}{L^4}\right)+TE\cdot\bar{z}\cdot\frac{\pi^2}{L^2}$$
$$=-\frac{\pi\cdot\rho\cdot D}{4\cdot U}\cdot\left[\begin{array}{l}C_D\cdot U^3+\frac{2}{\pi}\cdot\omega\cdot C_L\cdot U^2\cdot\bar{z}\cdot\sin(\omega\cdot t)+\frac{4}{\pi}\cdot C_D\cdot U^2\cdot\dot{\bar{z}}+\frac{1}{2}\cdot C_D\cdot\dot{\bar{y}}\cdot\left(\dot{\bar{z}}^2+\frac{1}{2}\cdot\dot{\bar{y}}^2\right)\\+\frac{1}{2}\cdot C_L\cdot U\cdot\dot{\bar{y}}\cdot\omega\cdot\bar{z}\cdot\sin(\omega\cdot t)+\frac{2}{3\cdot\pi}\cdot C_D\cdot\dot{\bar{y}}\cdot\dot{\bar{z}}^2+\frac{2}{3\cdot\pi}\cdot C_L\cdot\dot{\bar{y}}^2\cdot\sin(\omega\cdot t)^3\end{array}\right]$$

The symmetry of this problem ensures that the mean value of $\bar{y}$ is zero. In order to adjust the displacement $\bar{z}$ to one that has a mean value of zero the following change of variable to $\hat{z}$ is introduced,

$$\bar{z} = \hat{z} - \frac{\pi}{4} \cdot \frac{\rho \cdot D \cdot C_D \cdot U^2}{EI \cdot \frac{\pi^4}{L^4} + TE \cdot \frac{\pi^2}{L^2}}$$

With this alteration the governing equations become,

$$\left(m + \tilde{m}\right) \cdot \ddot{\bar{y}} + \xi \cdot 2\omega m y \cdot \dot{\bar{y}} \cdot EI + \left(TE \cdot \frac{\pi^4}{L^4} + y \cdot \frac{\pi^2}{L^2}\right) \cdot \bar{y}$$

$$= \frac{\pi \cdot \rho \cdot D}{4 \cdot U} \cdot \left[ \begin{array}{l} C_L \cdot U^3 \omega \sin\left(\omega \cdot t\right) - \frac{2}{\pi} U_D y \cdot \dot{\bar{y}}^2 \cdot C + \frac{4}{\pi} U_L z \cdot \sin\left(\omega \cdot t\right) \cdot \dot{\bar{y}} \\ + \frac{1}{2} \cdot C_L \cdot U \cdot \left(\dot{\hat{z}}^2 + \frac{1}{2} \cdot \dot{\bar{y}}^2\right) \cdot \sin\left(\omega \cdot t\right) - \frac{2}{3} C \cdot z_D \cdot \dot{\bar{y}}^3 \cdot \sin\left(\omega \cdot t\right) \cdot \dot{\hat{z}}^2 \cdot \left(\omega \cdot t\right) \end{array} \right]$$

$$\left(m + \tilde{m}\right) \cdot \ddot{\hat{z}} + \xi \cdot 2\omega m z \cdot \dot{\hat{z}} \cdot EI \cdot \hat{z} + \left(TE \cdot \frac{\pi^4}{L^4} + z \cdot \frac{\pi^2}{L^2}\right) \cdot \hat{z}$$

$$= -\frac{\pi \cdot \rho \cdot D}{4 \cdot U} \cdot \left[ \begin{array}{l} \frac{2}{\pi} \cdot C_L \cdot U^2 \cdot \dot{\bar{y}} \cdot \sin\left(\omega \cdot t\right) + \frac{4}{\pi} \cdot z_D \cdot \dot{\hat{z}}^2 \cdot C + U \cdot z_D \cdot \dot{\hat{z}} \cdot \left(\dot{\bar{y}}^2 + \frac{1}{2} \cdot \dot{\hat{z}}^2\right) \\ + \frac{1}{2} \cdot C_L \cdot U \cdot \dot{\bar{y}} \omega z \cdot \sin\left(\omega \cdot t\right) + \frac{2}{3 \cdot \pi} y_D \cdot \dot{\hat{z}} \cdot \dot{\bar{y}}^2 + \frac{2}{3 \cdot \pi} \cdot \sin\left(\omega \cdot t\right)^3 \cdot \left(\omega \cdot t\right) \end{array} \right]$$

## NUMERICAL SCHEME FOR SOLVING GOVERNING EQUATIONS

The last two equations of Section E are transformed to dimensionless variables before performing a numerical integration. The new, dimensionless variables are defined as follows,

$$Y = \frac{\omega \cdot \bar{y}}{U}$$

$$Z = \frac{\omega \cdot \hat{z}}{U}$$

$$\tau = \omega \cdot t$$

Also define the following notation,

$$\dot{\psi} \equiv \omega \cdot \psi_{,\tau}$$

$$\tilde{E} = EI \cdot \left(\frac{\pi}{L}\right)^4 + TE \cdot \left(\frac{\pi}{L}\right)^2$$

$$FAC = \frac{m + \tilde{m}}{m}$$

These changes convert the governing equations to the following form,

$$FAC \cdot Y_{,\tau\tau} + 2 \cdot \zeta \cdot Y_{,\tau} + \frac{\tilde{E}}{m \cdot \omega^2} \cdot Y = \frac{\pi}{4} \cdot \left(\frac{\rho \cdot D \cdot U}{m \cdot \omega}\right) \cdot \begin{bmatrix} -C_D \cdot \left(\frac{2}{\pi} \cdot Y_{,\tau} + \frac{1}{2} \cdot Y_{,\tau} \cdot Z_{,\tau} + \frac{2}{3 \cdot \pi} \cdot Y_{,\tau}^2\right) + \\ C_L \cdot \left(1 + \frac{4}{\pi} \cdot Z_{,\tau} + \frac{1}{4} \cdot Y_{,\tau}^2 + \frac{1}{2} \cdot Z_{,\tau}^2 + \frac{2}{3 \cdot \pi} \cdot Y_{,\tau}^2 \cdot Z_{,\tau}\right) \cdot \sin(\tau) \end{bmatrix}$$

$$FAC \cdot Z_{,\tau\tau} + 2 \cdot \zeta \cdot Z_{,\tau} + \frac{\tilde{E}}{m \cdot \omega^2} \cdot Z = \frac{\pi}{4} \cdot \left(\frac{\rho \cdot D \cdot U}{m \cdot \omega}\right) \cdot C_D - \frac{\pi}{4} \cdot \left(\frac{\rho \cdot D \cdot U}{m \cdot \omega}\right) \cdot \begin{bmatrix} C_D \cdot \left(1 + \frac{4}{\pi} \cdot Z_{,\tau} + \frac{1}{4} \cdot Y_{,\tau}^2 + \frac{1}{2} \cdot Z_{,\tau}^2 + \frac{2}{3 \cdot \pi} \cdot Y_{,\tau}^2 \cdot Z_{,\tau}\right) + \\ C_L \cdot \left(\frac{2}{\pi} \cdot Y_{,\tau} + \frac{1}{2} \cdot Y_{,\tau} \cdot Z_{,\tau} + \frac{2}{3 \cdot \pi} \cdot Y_{,\tau}^2\right) \cdot \sin(\tau) \end{bmatrix}$$

The left-hand side of the first equation indicates the fundamental natural frequency, $\omega_n$, is given by,

$$\omega_n = \sqrt{\frac{\tilde{E}}{FAC \cdot m}}$$

Since only the resonant case is being considered and the excitation is from the vortex shedding, the Strouhal number also determines the natural frequency as,

$$\omega_n = \frac{2 \cdot \pi \cdot U \cdot S}{D}$$

In order for the last two equations to be consistent, the value of $\omega_n$ from the second $\omega_n$ equation is used to determine the value of L in $\tilde{E}$ so that,

$$L = \frac{\pi}{\sqrt{-\frac{TE}{EI} + \sqrt{\left(\frac{TE}{EI}\right)^2 + 4 \cdot \frac{(FAC \cdot \omega_n)^2}{EI}}}} = \frac{\pi}{\sqrt{-\frac{TE}{EI} + \sqrt{\left(\frac{TE}{EI}\right)^2 + \frac{16 \cdot \pi^2}{EI} \cdot \left(\frac{FAC \cdot U \cdot S}{D}\right)^2}}}$$

And the governing equations become,

$$FAC \cdot Y_{,\tau\tau} + 2 \cdot \zeta \cdot Y_{,\tau} + FAC \cdot Y = \frac{\pi}{4} \cdot \left(\frac{\rho \cdot D \cdot U}{m \cdot \omega}\right) \cdot \left[\begin{array}{l} -C_D \cdot \left(\frac{2}{\pi} \cdot Y_{,\tau} + \frac{1}{2} \cdot Y_{,\tau} \cdot Z_{,\tau} + \frac{2}{3 \cdot \pi} \cdot Y_{,\tau}^2\right) + \\ C_L \cdot \left(1 + \frac{4}{\pi} \cdot Z_{,\tau} + \frac{1}{4} \cdot Y_{,\tau}^2 + \frac{1}{2} \cdot Z_{,\tau}^2 + \frac{2}{3 \cdot \pi} \cdot Y_{,\tau}^2 \cdot Z_{,\tau}\right) \cdot \sin(\tau) \end{array}\right]$$

$$FAC \cdot Z_{,\tau\tau} + 2 \cdot \zeta \cdot Z_{,\tau} + FAC \cdot Z = \frac{\pi}{4} \cdot \left(\frac{\rho \cdot D \cdot U}{m \cdot \omega}\right) \cdot C_D - \frac{\pi}{4} \cdot \left(\frac{\rho \cdot D \cdot U}{m \cdot \omega}\right) \cdot \left[\begin{array}{l} C_D \cdot \left(1 + \frac{4}{\pi} \cdot Z_{,\tau} + \frac{1}{4} \cdot Y_{,\tau}^2 + \frac{1}{2} \cdot Z_{,\tau}^2 + \frac{2}{3 \cdot \pi} \cdot Y_{,\tau}^2 \cdot Z_{,\tau}\right) + \\ C_L \cdot \left(\frac{2}{\pi} \cdot Y_{,\tau} + \frac{1}{2} \cdot Y_{,\tau} \cdot Z_{,\tau} + \frac{2}{3 \cdot \pi} \cdot Y_{,\tau}^2\right) \cdot \sin(\tau) \end{array}\right]$$

Note that the steady-state solution for the dimensionless displacements may be found when FAC, $\zeta$, $\frac{\rho \cdot D \cdot U}{m \cdot \omega_n}$, $C_D$ and $C_L$ are specified. The method used here for finding the steady-state solution is to estimate a set of initial conditions (since the actual values are

unknown) and numerically integrate them until the displacements become essentially cyclic. The cyclic behavior is the steady-state solution. For the illustrative problems presented below the steady-state is reached in less than 10 cycles for Y. The estimates for the initial conditions are,

$$\text{At } \tau = 0 \qquad Y = 0, \qquad Y_{,\tau} = \frac{\omega_n{}^2 \cdot D}{U} \qquad Z = 0.05 \cdot \frac{\omega_n \cdot D}{U} \qquad Z_{,\tau} = 0$$

## ILLUSTRATIVE EXAMPLE

INPUT DATA FOR PROGRAM VIVN2:

| | | |
|---|---|---|
| EI | = bending stiffness, lbf-in$^2$ | = 16.1E6 |
| m | = mass per unit length, lbf-sec$^2$/in$^2$ | = 0.001 |
| TE | = effective tensile force, lbf | = 500. |
| D | = diameter, in | = 2.00 |
| U | = fluid velocity, in/sec | = 24.0 |
| $\rho$ | = fluid mass density, lbf-sec$^2$/in$^4$ | = 0.960E-4 |
| $\nu$ | = fluid kinematic viscosity, in$^2$/sec | = 0.00160 |
| $C_D$ | = fluid drag coefficient | = 1.20 |
| $C_L$ | = fluid lift coefficient | = 1.00 |
| $\zeta$ | = structural damping coefficient | = 0.00 |

INTERMEDIATE OUTPUT DATA FROM PROGRAM VIVN2

| | | |
|---|---|---|
| $\omega_n$ | = fundamental, circular natural frequency, rad/sec | = 14.36 |
| FREQ | = frequency, cyc/sec | = 2.285 |
| L | = length of half sine wave, in | = 293.6 |
| RE | = Reynolds' number | = 0.3000E5 |
| STN | = Strouhal number | = 0.1905 |
| ROM | $= \dfrac{\rho \cdot D \cdot U}{m \cdot \omega_n}$ | = 0.3209 |
| ESD | $= \dfrac{\tilde{E}}{m \cdot \omega_n^{\,2}}$ | = 1.302 |
| FAC | $= \dfrac{m + \tilde{m}}{m}$ | = 1.302 |

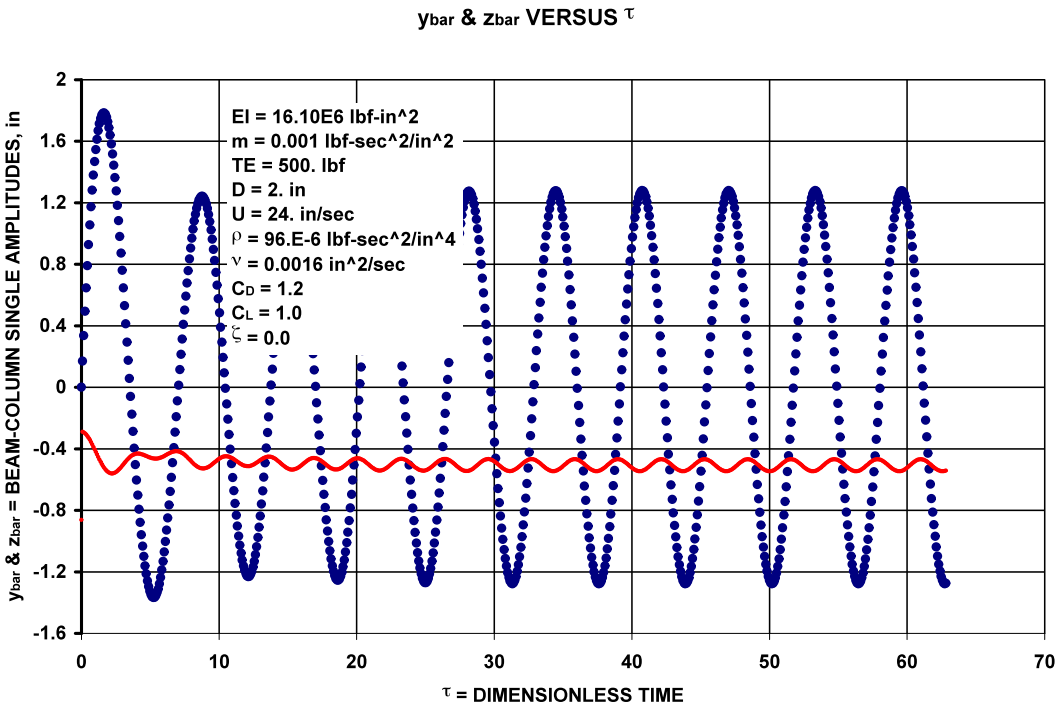
ybar & zbar VERSUS τ
EI = 16.10E6 lbf-in^2
m = 0.001 lbf-sec^2/in^2
TE = 500. lbf
D = 2. in
U = 24. in/sec
ρ = 96.E-6 lbf-sec^2/in^4
ν = 0.0016 in^2/sec
CD = 1.2
CL = 1.0
ζ = 0.0
ybar & zbar = BEAM-COLUMN SINGLE AMPLITUDES, in
τ = DIMENSIONLESS TIME
2
1.6
1.2
0.8
0.4
0
-0.4
-0.8
-1.2
-1.6
0
10
20
30
40
50
60
70

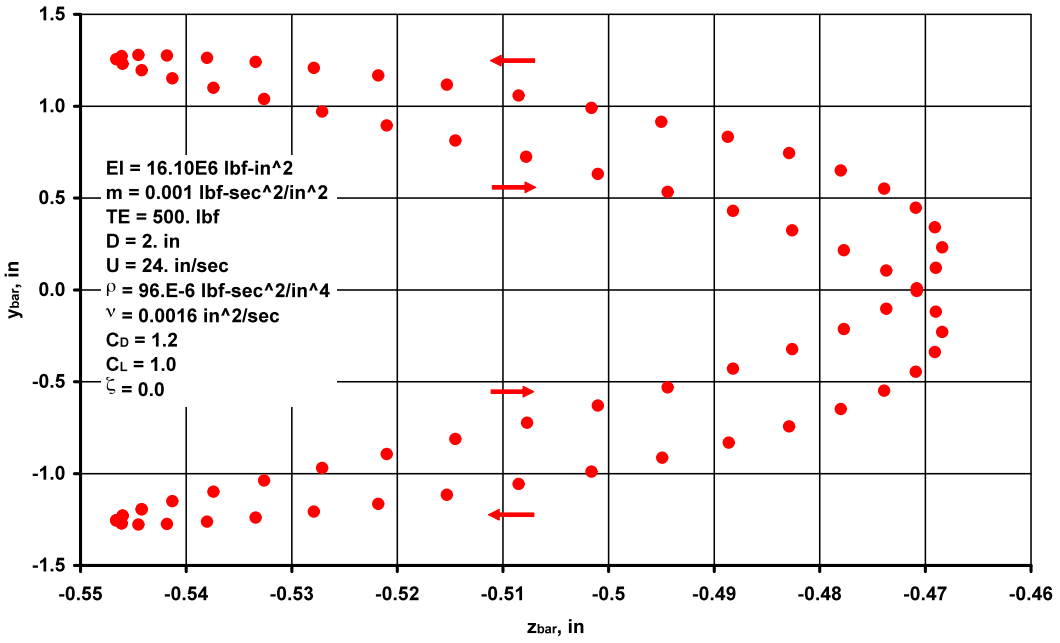
zbar VERSUS ybar
EI = 16.10E6 lbf-in^2
m = 0.001 lbf-sec^2/in^2
TE = 500. lbf
D = 2. in
U = 24. in/sec
ρ = 96.E-6 lbf-sec^2/in^4
ν = 0.0016 in^2/sec
CD = 1.2
CL = 1.0
ζ = 0.0
ybar, in
zbar, in
1.5
1.0
0.5
0.0
-0.5
-1.0
-1.5
-0.55
-0.54
-0.53
-0.52
-0.51
-0.5
-0.49
-0.48
-0.47
-0.46

The illustrative example reported above is for a steel tube with OD = 2.0 in and ID = 1.5 in, under an effective tension of 500 lbf submerged in water at 65 $^{o}$F and flowing at 2 ft/sec. The standard value of $C_D = 1.2$ was used while the speculated value of $C_L = 1.0$ was chosen. The first illustrative example figure above shows the fundamental frequency of vibration for the lateral motion is 2.285 cyc/sec while the fundamental frequency of vibration for the axial motion is 4.57 cyc/sec. The amplitude of lateral motion is 1.4 inches which is 70 % of the OD.

Reference 2, Page 71, Table 3-2 gives results of earlier analyses for $\frac{\overline{y}_{max}}{D}$ at resonance. For this illustrative case the applicable results are,

Wake Oscillator Model[7] $\frac{\overline{y}_{max}}{D} = 1.576$

Griffen and Ramberg Model[8] $\frac{\overline{y}_{max}}{D} = 1.490$

Sarpkaya Model[9] $\frac{\overline{y}_{max}}{D} = 1.509$

All of these predictions are more than twice the prediction of $\frac{\overline{y}_{max}}{D} = 0.70$ from the illustrative case. The current analysis has a number of assumptions that make its predictions subject to error. In addition, it is the only analysis using $C_L = 1.0$. An increase in the value of $C_L$ or a decrease in the value of $C_D$ will increase $\frac{\overline{y}_{max}}{D}$. Since the value of $C_D$ has been established experimentally within close limits for a Reynolds' number of 30,000, it is not likely to be the primary source of error. An influence that is not considered in this work is that the drag coefficient can be increased substantially owing to the laterally induced motion, Reference 2, Section 3.3. Since an attempt to account for this phenomenon would worsen the spread in the current results and the three given above, it is not pursued. If the value of $C_D = 1.2$ is accepted, then the value of $C_L$ can be adjusted to match the above results. When this procedure is followed, $C_L$ must be greater than 2.0 to match the three results above. This high value for $C_L$ seems to the author to be inconsistent with the usual explanation for the lift phenomenon for the problem. The usual explanation is that a region of stagnation moves from side to side of the beam-column as the lateral motion proceeds. The region of stagnation should have, approximately, the free stream pressure.

The second figure for the illustrative problem is a Lissajous figure of the y and z directions motion. This is the type of figure that is often measured for the motion; see Reference 2, Page 94, Figure 3-31. This figure shows that the period of axial motion is half that of the lateral motion as predicted by Program VIVN2.

## SOME INFLUENCES OF PARAMETER VARIATIONS

In this section the illustrative problem in Section F is used as a base case and one parameter is varied to obtain its influence on the solution. This procedure is followed for each of the following parameters with their values for the base case given below,

$\frac{\rho \cdot D \cdot U}{m \cdot \omega}$ = 0.3209

$C_D$ = 1.20

$C_L$ = 1.00

$\zeta$ = 0.00

In the figures below, $\Delta Z$ is the maximum variation of Z in the steady-state while ZMEAN is the mean value of Z in the steady-state. $Y_{max}$ and $\Delta Z/2$ are single peak amplitudes and $y_{bar} = \bar{y}$. All results in this section are for steady state conditions.

1. $\frac{\rho \cdot D \cdot U}{m \cdot \omega}$ variation

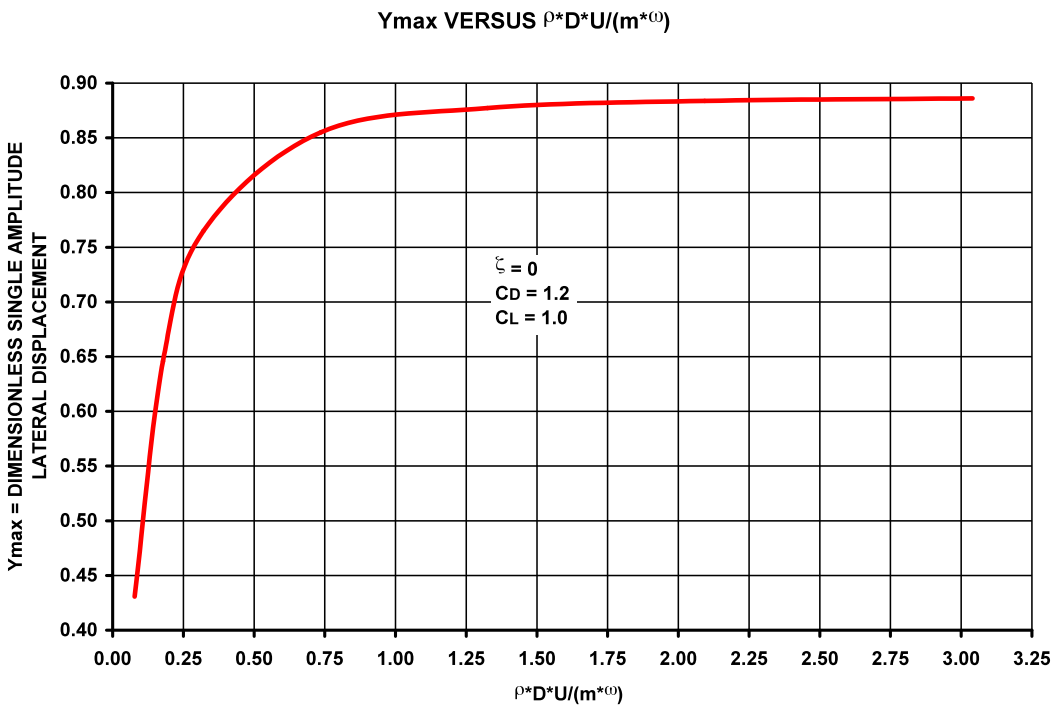

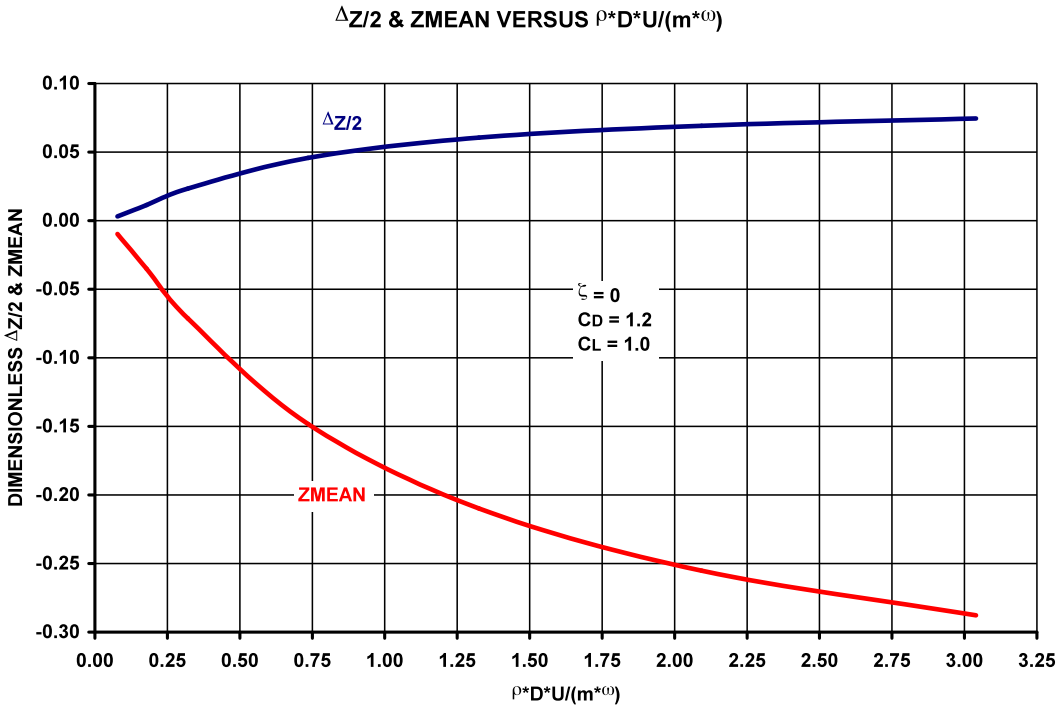
ΔZ/2 & ZMEAN VERSUS ρ*D*U/(m*ω)
DIMENSIONLESS ΔZ/2 & ZMEAN
ΔZ/2
ZMEAN
ζ = 0
CD = 1.2
CL = 1.0
0.10
0.05
0.00
-0.05
-0.10
-0.15
-0.20
-0.25
-0.30
0.00 0.25 0.50 0.75 1.00 1.25 1.50 1.75 2.00 2.25 2.50 2.75 3.00 3.25
ρ*D*U/(m*ω)

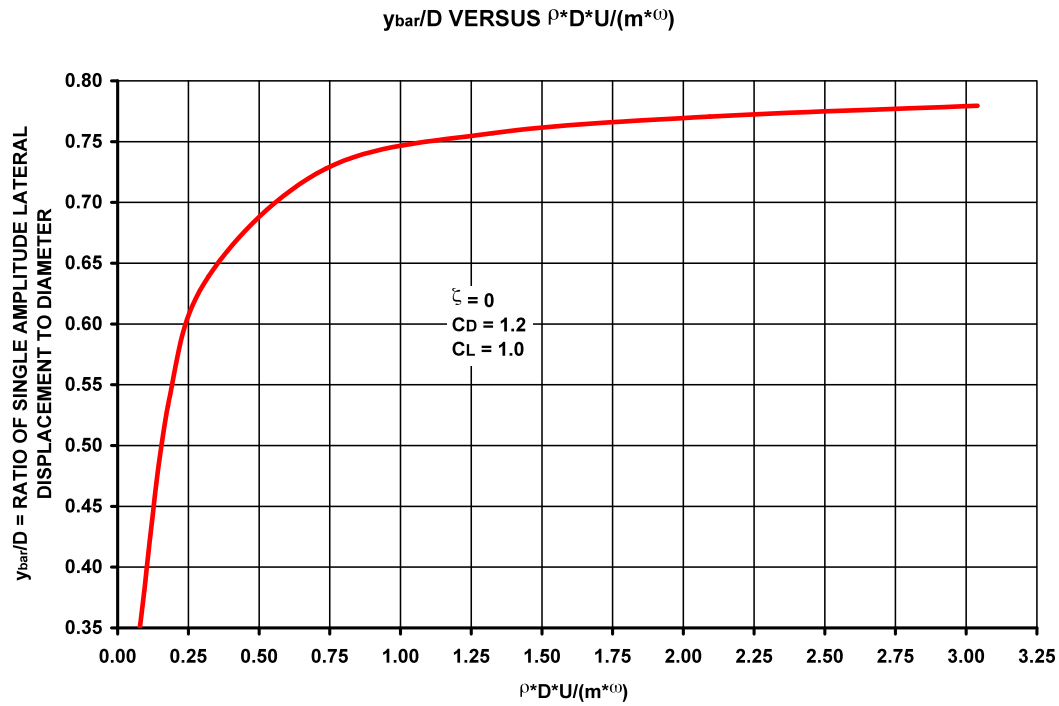
ybar/D VERSUS ρ*D*U/(m*ω)
ybar/D = RATIO OF SINGLE AMPLITUDE LATERAL DISPLACEMENT TO DIAMETER
ζ = 0
CD = 1.2
CL = 1.0
0.80
0.75
0.70
0.65
0.60
0.55
0.50
0.45
0.40
0.35
0.00 0.25 0.50 0.75 1.00 1.25 1.50 1.75 2.00 2.25 2.50 2.75 3.00 3.25
ρ*D*U/(m*ω)

**2.** $C_D$ variation

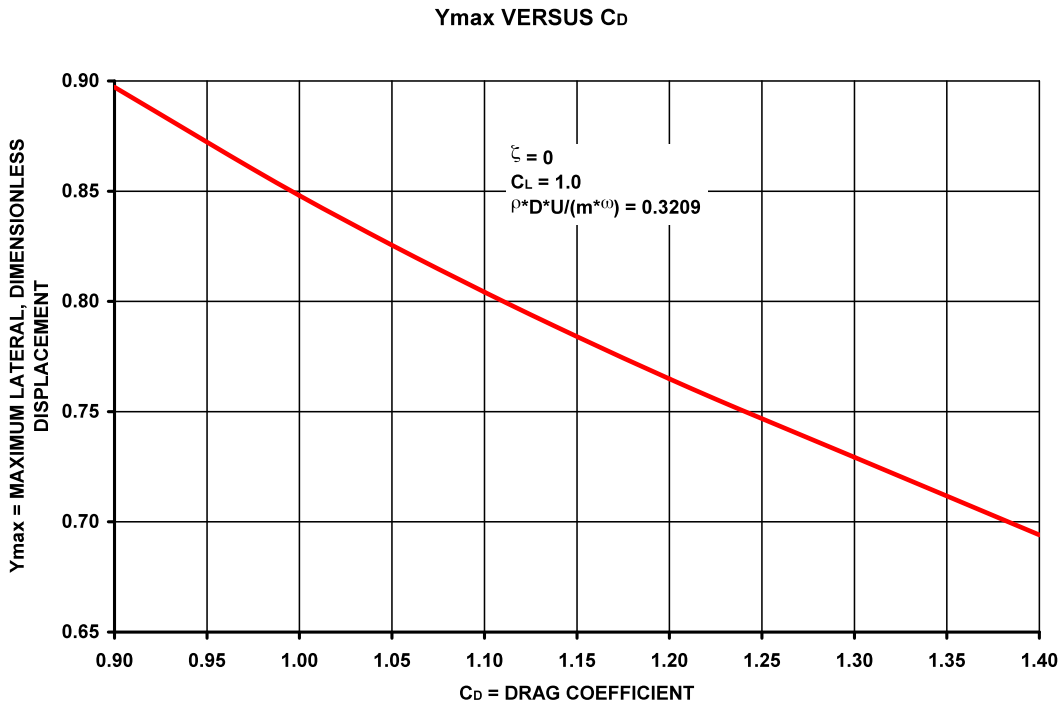


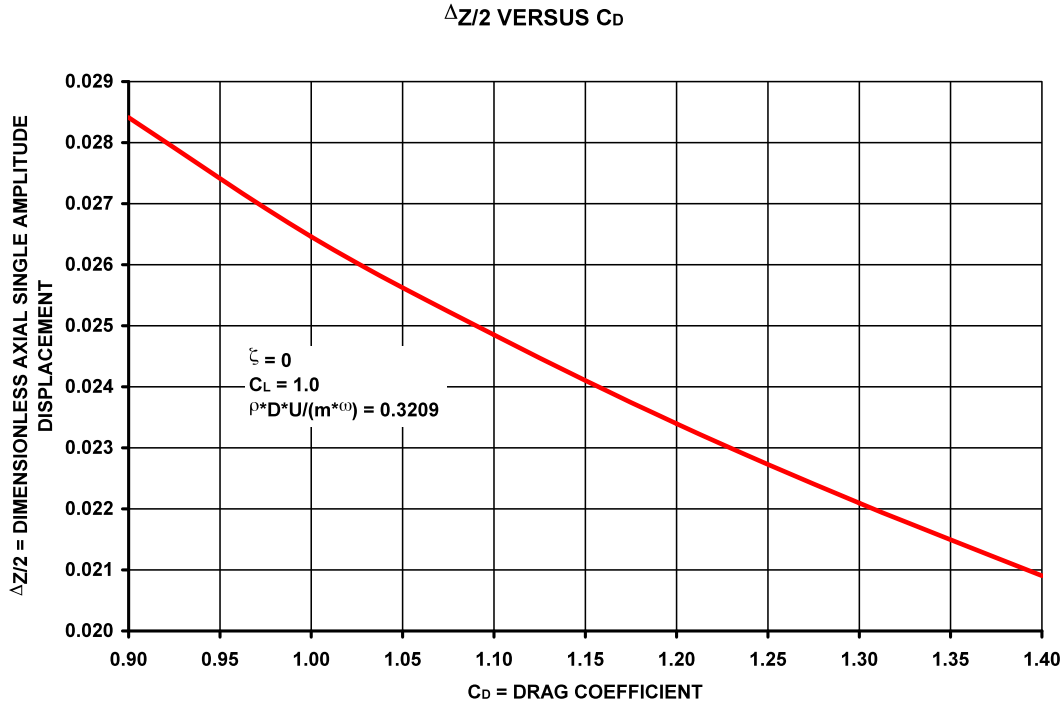

ZMEAN VERSUS $C_D$

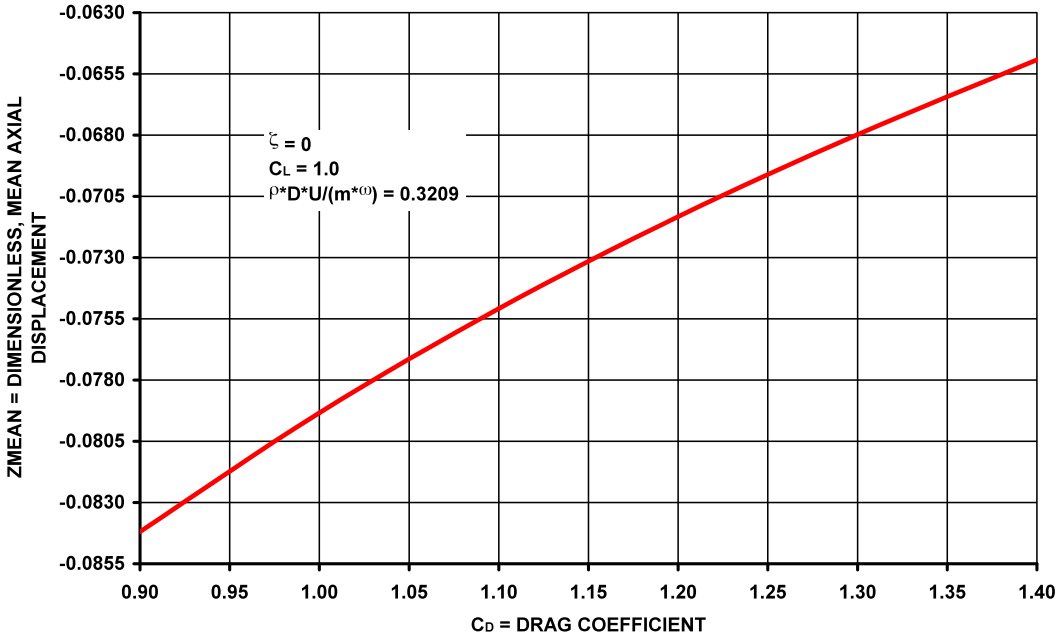


$y_{bar}/D$ VERSUS $C_D$

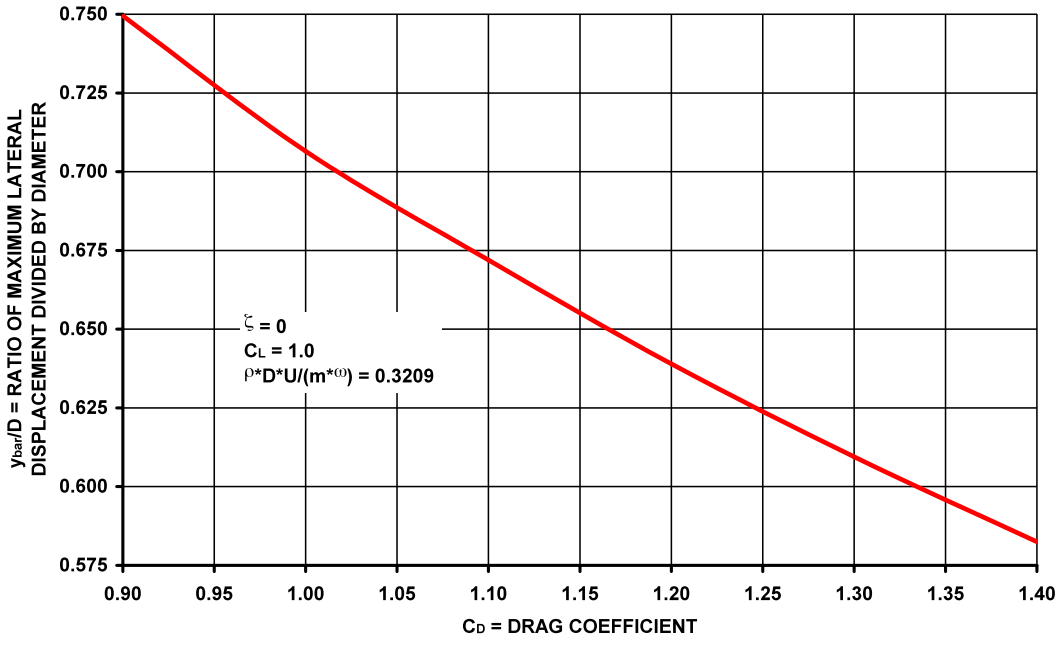

**3.** $C_L$ variation

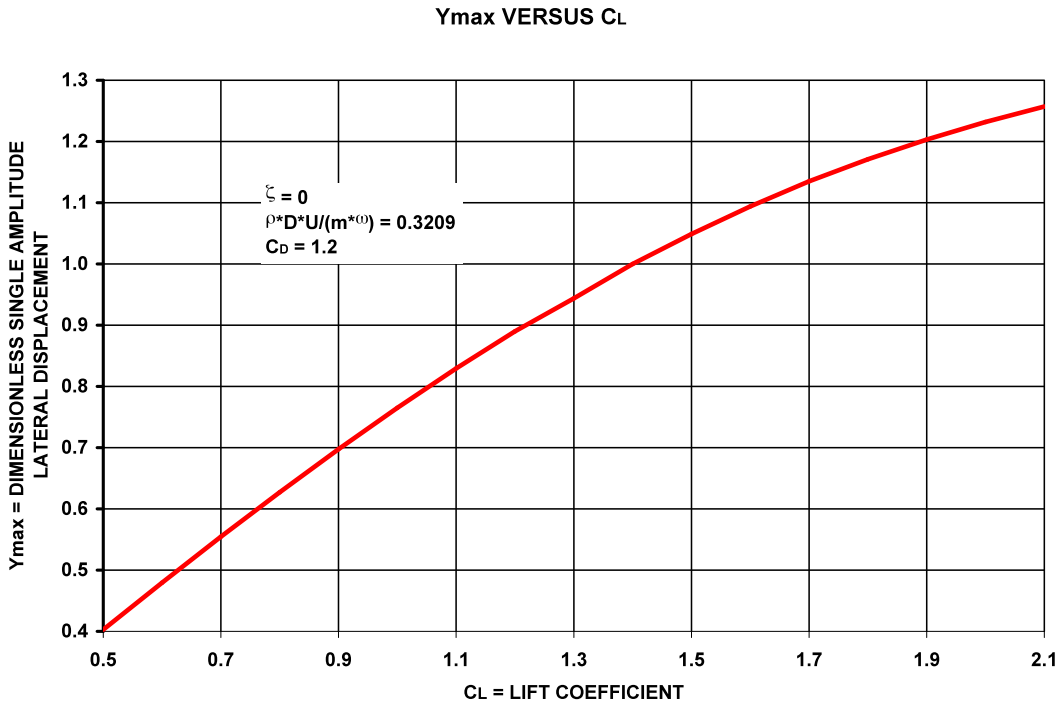


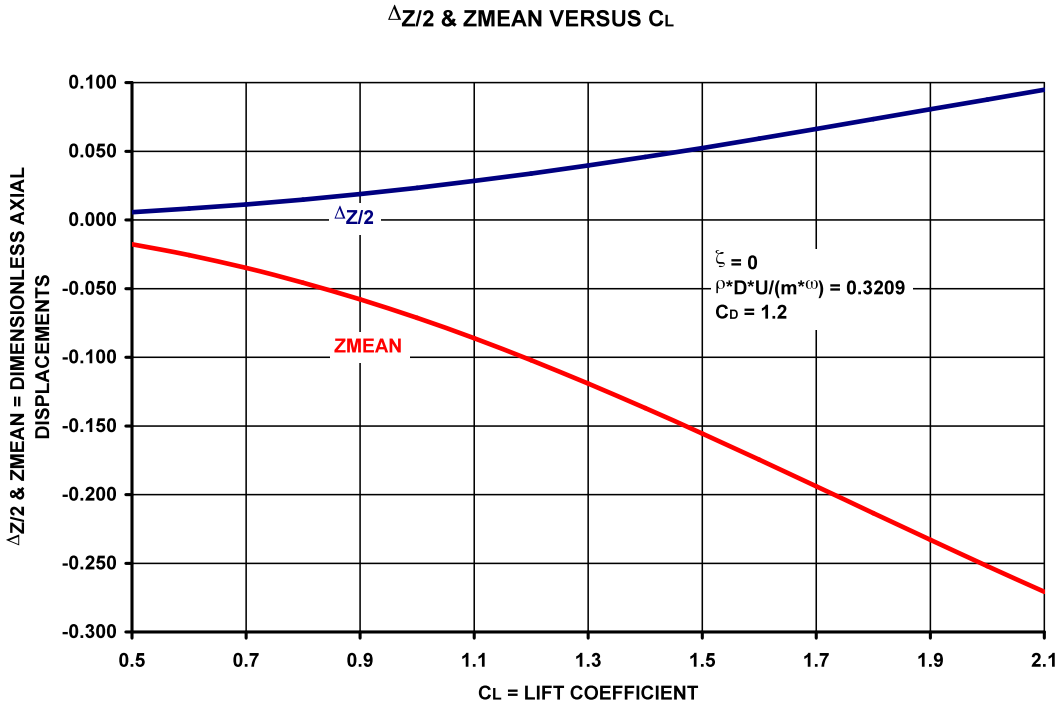

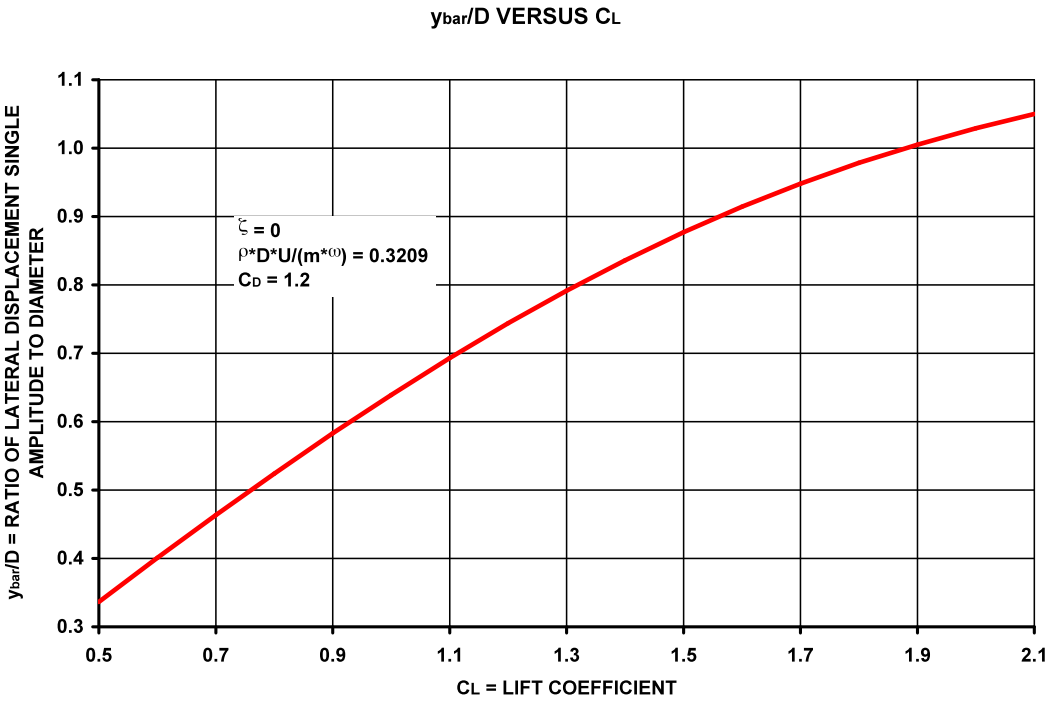
ybar/D VERSUS CL
ybar/D = RATIO OF LATERAL DISPLACEMENT SINGLE AMPLITUDE TO DIAMETER
1.1
1.0
0.9
0.8
0.7
0.6
0.5
0.4
0.3
ζ = 0
ρ*D*U/(m*ω) = 0.3209
CD = 1.2
0.5
0.7
0.9
1.1
1.3
1.5
1.7
1.9
2.1
CL = LIFT COEFFICIENT

4. ζ variation

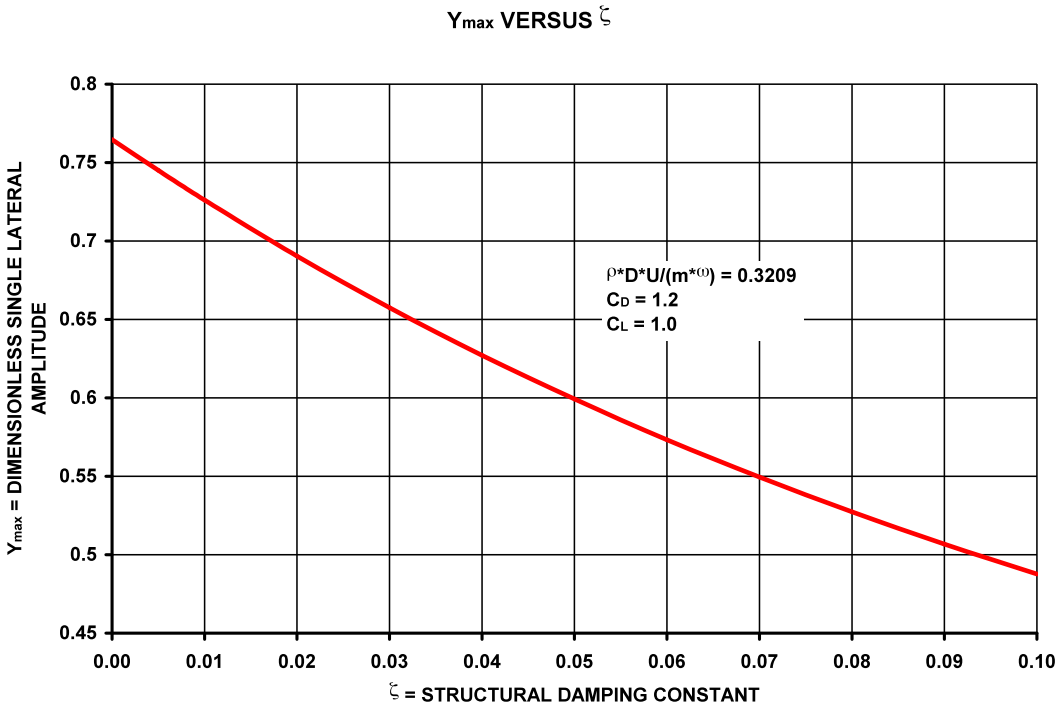


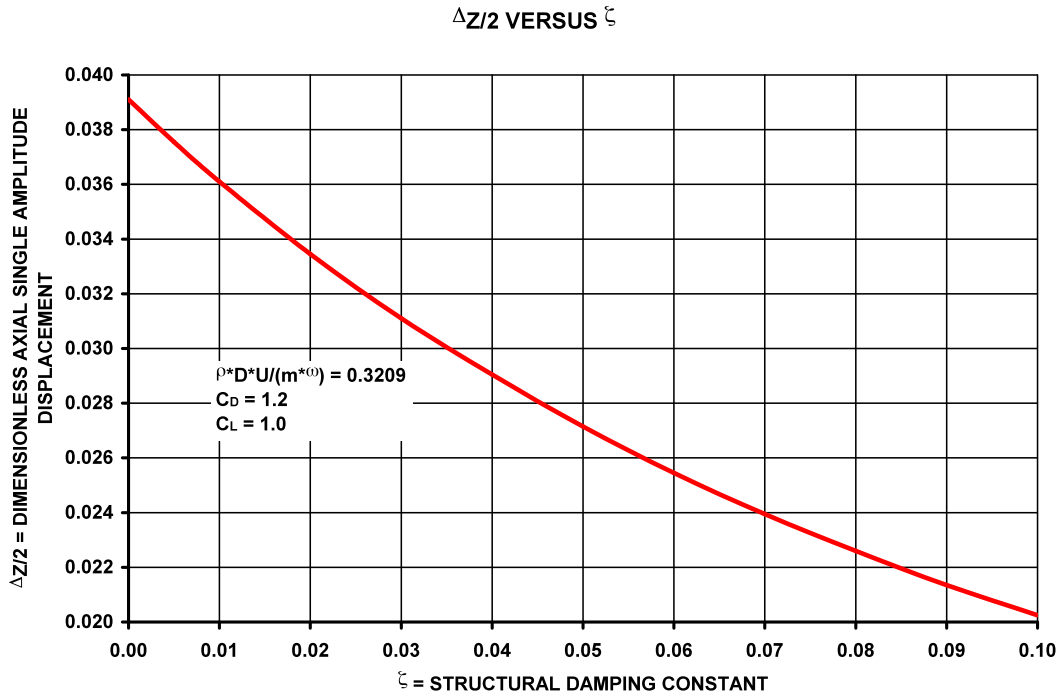

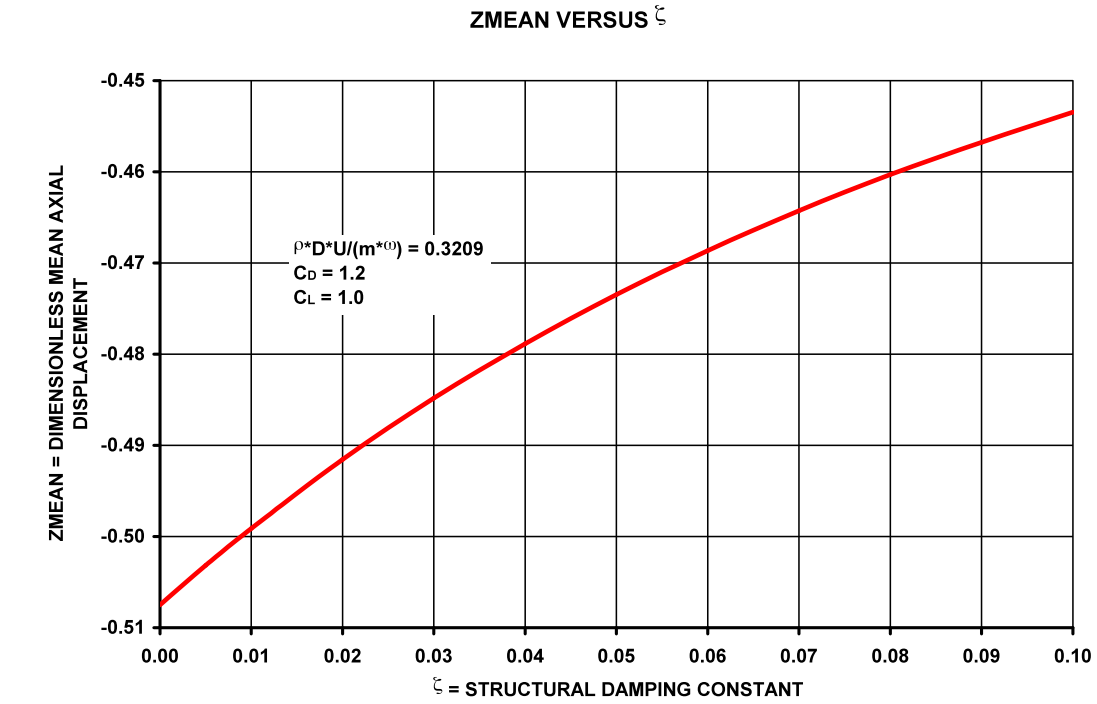
ZMEAN VERSUS ζ
ZMEAN = DIMENSIONLESS MEAN AXIAL DISPLACEMENT
-0.45
-0.46
-0.47
-0.48
-0.49
-0.50
-0.51
ρ*D*U/(m*ω) = 0.3209
CD = 1.2
CL = 1.0
0.00
0.01
0.02
0.03
0.04
0.05
0.06
0.07
0.08
0.09
0.10
ζ = STRUCTURAL DAMPING CONSTANT

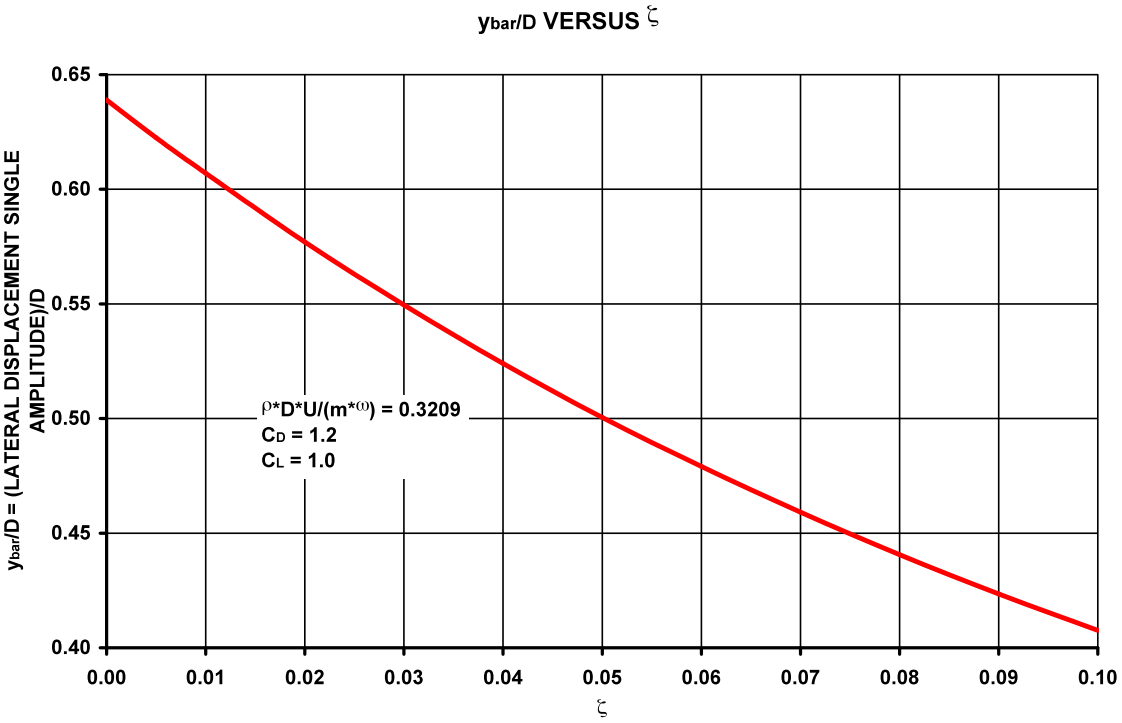
ybar/D VERSUS ζ
ybar/D = (LATERAL DISPLACEMENT SINGLE AMPLITUDE)/D
0.65
0.60
0.55
0.50
0.45
0.40
ρ*D*U/(m*ω) = 0.3209
CD = 1.2
CL = 1.0
0.00
0.01
0.02
0.03
0.04
0.05
0.06
0.07
0.08
0.09
0.10
ζ

**SOME OBSERVATIONS**

1. Vortex-induced vibration for a very elementary case is modeled using forces on a simply supported beam-column subjected to a uniform fluid flow normal to the beam-column axis. The forces are determined using the Morison equation[10]. The analysis includes second order terms in the velocity components. Beam-column displacements both parallel and perpendicular to the flow direction are included.

2. The results are qualitatively OK. They should be helpful in designing experiments and estimating influences of parameter changes.

3. The predictions for the lateral motion amplitudes are disappointing when compared to reported experimental values. The predictions presented above show that the lateral motion amplitudes are strongly dependent on the lift coefficient. In Reference 2, Figure 3-16, Page 64 the values of the experimental lift coefficients are all less than 1.4 with an average closer to 0.8. The illustrative example used $C_L = 1.0$ and predicts a lateral motion amplitude less than one half of the results cited on Page 14 above. The figure on Page 20 shows that this analysis requires a value for $C_L$ of about 2.0 to match the Page 14 results.

4. In order to evaluate the importance of including the axial motion of the beam-column in the analysis, the above formulation was altered to set the axial displacement of the beam-column to a constant in the steady-state. The same input data to this modified program was used that was used for the top figure on Page 14 above. The lateral displacement amplitude as a function of dimensionless time is shown below. Comparison of this figure with the top figure on Page 14 shows that the steady-state solutions are virtually the same.

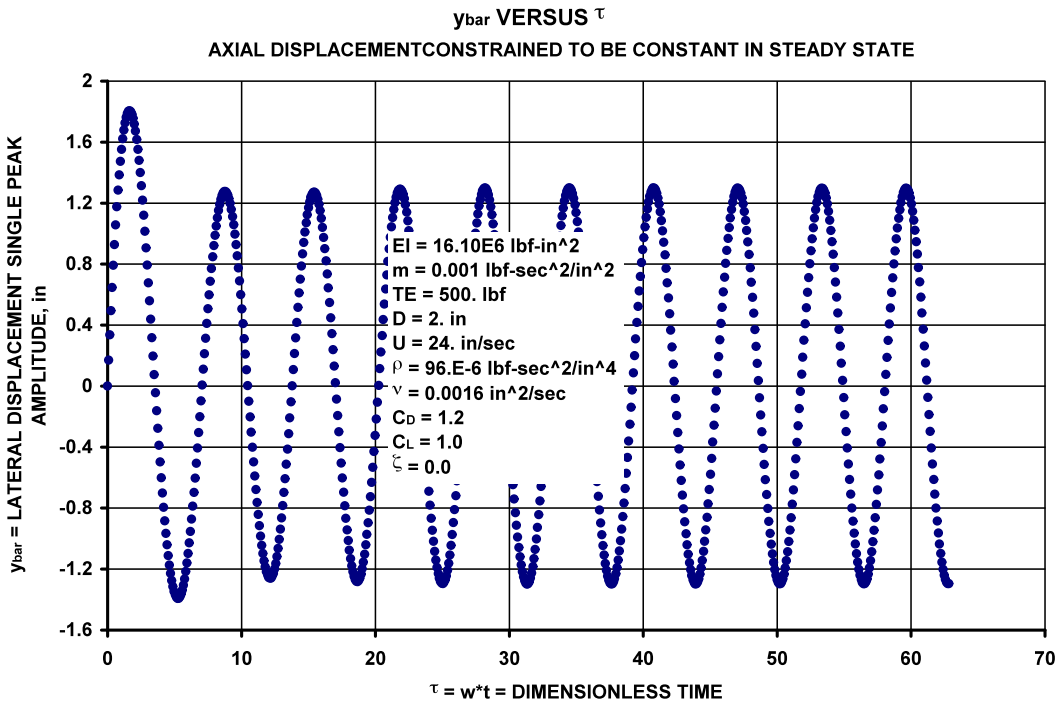


The governing equation for the above figure is,

$$FAC\cdot Y_{,\tau\tau} + 2\cdot\zeta\cdot Y_{,\tau} + FAC\cdot Y = \frac{\pi}{4}\cdot\left(\frac{\rho\cdot D\cdot U}{m\cdot\omega}\right)\cdot\left[-C_D\cdot\left(\frac{2}{\pi}\cdot Y_{,\tau} + \frac{2}{3\cdot\pi}\cdot Y_{,\tau}^{\,2}\right) + C_L\cdot\left(1+\frac{1}{4}\cdot Y_{,\tau}^{\,2}\right)\cdot\sin(\tau)\right]$$

At resonant conditions in the Harmonic Model described in Reference 2, Section 3.5.1, pp. 61-67, this equation is linearized and $C_D$ is set to zero. The result is,

$$\left.\overline{y}\right|_{\text{resonance}} = \frac{\pi}{8\cdot\zeta}\cdot\frac{\rho\cdot D\cdot U^2}{FAC\cdot m\cdot\omega_n^{\,2}}\cdot C_L$$

Note that the amplitude is inversely proportional to ζ. The amplitude is predicted to be infinite at resonance when the beam-column damping is set to zero. This result is not useful in the current study and it demonstrates that non-linear influences must be included in order to have a useful analysis.

5. The vortex shedding phenomenon has been studied experimentally. The vortex at resonance normally separates from the upper side of the cylinder when the peak lateral displacement is reached and the new vortex immediately starts forming on the lower side of the cylinder. In many resonant analyses the lateral force imposed on the cylinder by the fluid is assumed to be sinusoidal in time. It seems to the author that the sinusoidal assumption could legitimately be questioned. As a result, the calculation procedure described above (starting on page 10) was altered to change the sinusoidal wave to a square wave. The salient results are shown in the figures below.

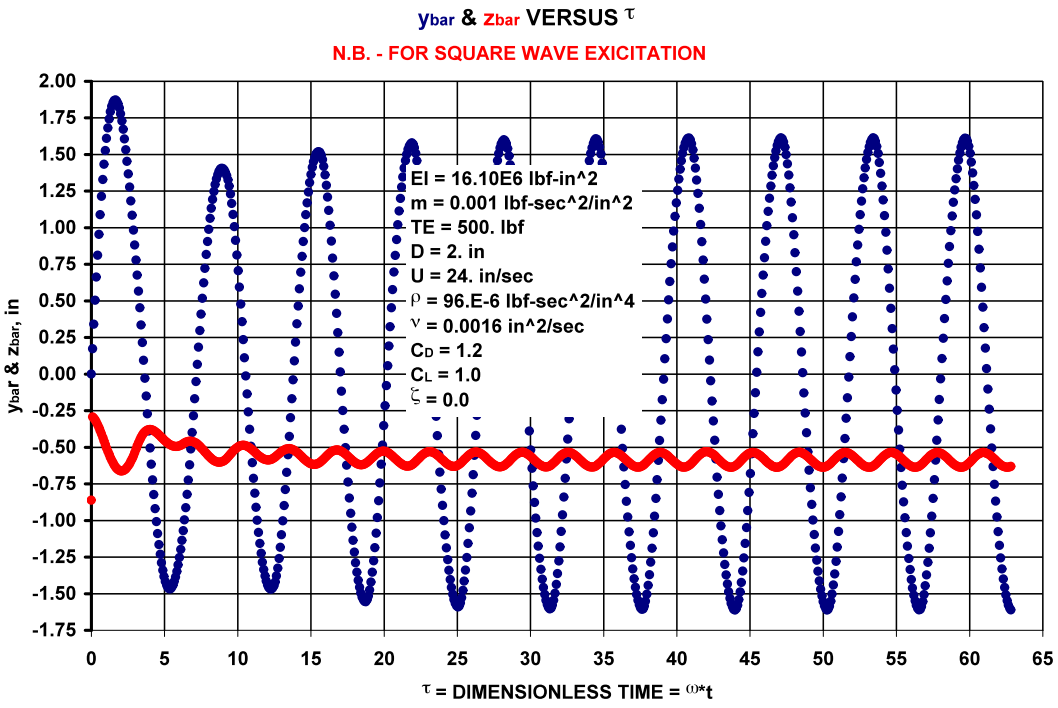

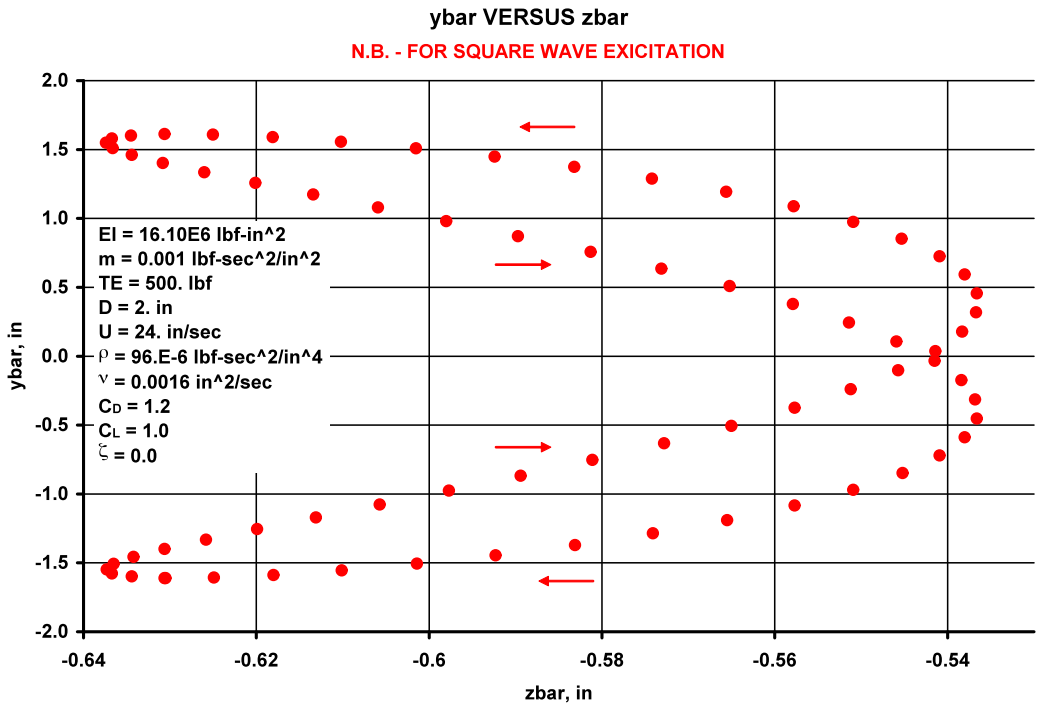
ybar VERSUS zbar
N.B. - FOR SQUARE WAVE EXICITATION
EI = 16.10E6 lbf-in^2
m = 0.001 lbf-sec^2/in^2
TE = 500. lbf
D = 2. in
U = 24. in/sec
ρ = 96.E-6 lbf-sec^2/in^4
ν = 0.0016 in^2/sec
CD = 1.2
CL = 1.0
ζ = 0.0
ybar, in
zbar, in
2.0
1.5
1.0
0.5
0.0
-0.5
-1.0
-1.5
-2.0
-0.64
-0.62
-0.6
-0.58
-0.56
-0.54

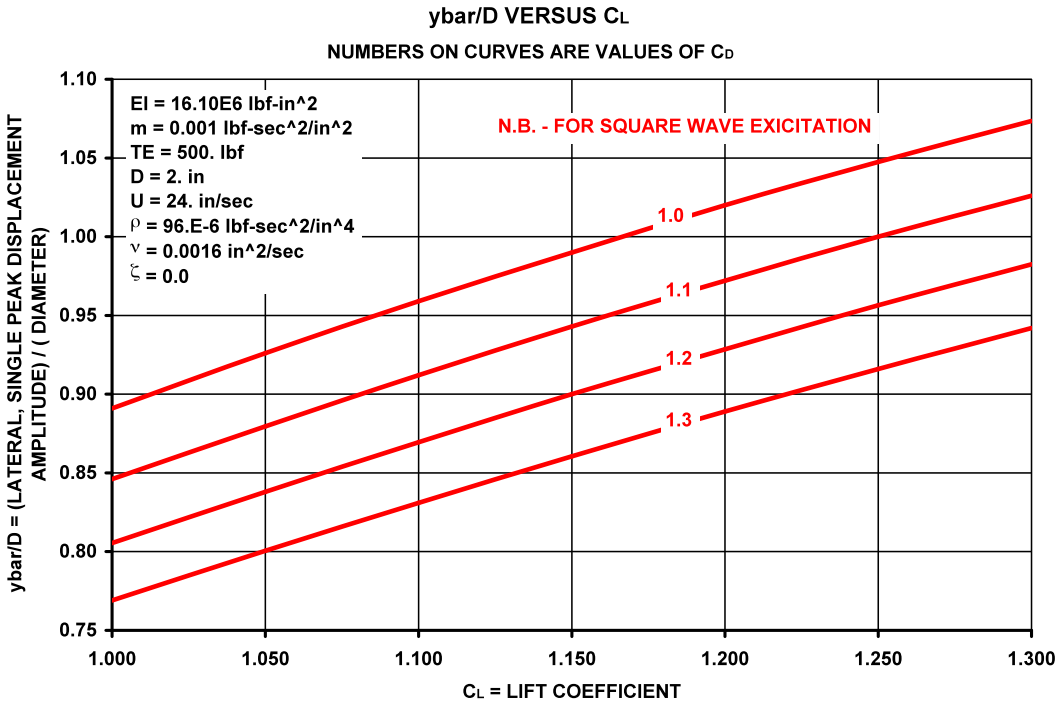
ybar/D VERSUS CL
NUMBERS ON CURVES ARE VALUES OF CD
N.B. - FOR SQUARE WAVE EXICITATION
EI = 16.10E6 lbf-in^2
m = 0.001 lbf-sec^2/in^2
TE = 500. lbf
D = 2. in
U = 24. in/sec
ρ = 96.E-6 lbf-sec^2/in^4
ν = 0.0016 in^2/sec
ζ = 0.0
1.0
1.1
1.2
1.3
ybar/D = (LATERAL, SINGLE PEAK DISPLACEMENT AMPLITUDE) / ( DIAMETER)
CL = LIFT COEFFICIENT
1.10
1.05
1.00
0.95
0.90
0.85
0.80
0.75
1.000
1.050
1.100
1.150
1.200
1.250
1.300

The above figure shows that the square wave forcing function yields predictions that are more in line with published experimental results than the sinusoidal forcing function.

## CONCLUSIONS

The initial analysis presented above shows that an elementary examination of a vortex-induced vibration problem using a long beam-column, classical fluid mechanics methods and contemporary modeling for the lift coefficient does not predict results for the deflection amplitude normal to the flow direction that agree with experimental results. The lateral amplitude predicted by the initial analysis is about one half its measured value.

An attempt to understand this disappointing result is presented above. The attempt is based on questioning the contemporary modeling of the lift coefficient. A common assumption for the lift coefficient model is to express the lift force as proportional to the stagnation pressure multiplied by the projected area, a lift coefficient and a sinusoidal variation at the vortex shedding frequency (based on the usual, empirical Strouhal Number formulation). Both von Karman's conjecture of $C_L = 1.0$ and measured results indicate the lift coefficient should be about one. The initial analysis used this formulation with the lift coefficient set equal to one.

For the drag model the physical description is that at the front of the cylinder is close to the stagnation pressure while the rear of the cylinder has a stalled region whose pressure is close to the free stream pressure. The lift force model has complications that are not present in the drag model. A casual consideration indicates that, unlike an airfoil, the symmetry of the lateral flow would not develop a lift force. In order to have a lift force the stalled region at the back of the cylinder must move laterally as the vortices are shed. The motion of the stalled region causes an oscillating lateral force on the cylinder. The side of the cylinder opposing the moving stalled region has a surface pressure below that of the free stream pressure. This reduced pressure can be estimated using the potential flow solution for flow normal to a stationary circular cylinder. Let a be the radius of the cylinder, r the generic radius and θ the angle measured to the flow direction. The free stream velocity is $V_O$ and then the velocity components are,

$V_x$ = fluid velocity component parallel to the flow $= V_O \cdot \left(1 - \frac{a^2}{r^2} \cdot \cos(2 \cdot \theta)\right)$

$V_y$ = fluid velocity component normal to flow $= -V_O \cdot \frac{a^2}{r^2} \cdot \sin(2 \cdot \theta)$

Consequently, the velocity at the cylinder surface and $\theta = \frac{1}{2} \cdot \pi$ is $2 \cdot V_O$ so the pressure decrease from the free stream value is $2 \cdot \rho \cdot V_O^2$. Taking the free stream pressure on one side of the cylinder and the (free stream pressure - $2 \cdot \rho \cdot V_O^2$) on the other gives an upper bound on the lift coefficient of $C_L = 4$. If the value of β (see Pages 3 & 4) is assumed to be $\frac{1}{4} \cdot \pi$, the maximum value of $C_L$ would be expected to be about 2.8. This maximum value is greater than the maximum measured value of < 1.2.

Based on this discussion of the value of $C_L$, the failure of the prediction of deflection amplitude normal to the flow direction may be an indication that the sinusoidal forcing function may not be properly modeled. In order to investigate this notion the sinusoidal forcing function was replaced by a square wave forcing function. The results of this change are given by the two figures on Page 27. The lower figure shows that the results of this second analysis are in better agreement with measurements than the initial analysis.

A final observation is that there is considerable variation in measured lift forces on a stationary cylinder; see Reference 2, Figure 3-16, Page 64. It may be that the rigidity of the cylinder in the direction normal to the free stream direction could influence the lift coefficient. If this is the case, force measurements should be made under resonant conditions.

The results presented here on Page 27 for square wave excitation are the results that are closer to measurements. This does not ensure that the true physical description of the model is consistent with the square wave model. The square wave model can be considered only to be a model that gives reasonable agreement with measurements that are better than the sinusoidal excitation model.

**REFERENCES**


1. J. P. Den Hartog, "Recent Technical Manifestations of von Karman's Vortex Wake," Proceedings of the National Academy of Sciences, v. 40, pp. 155-157, 1954
2. Robert D. Blevins, *Flow-Induced Vibrations*, Second Edition, Krieger Publishing Company, Malabar, Florida, 1994
3. J. Kim Vandiver and Li Li, "SHEAR7 Program Theoretical Manual," Department of Ocean Engineering, Massachusetts Institute of Technology, 2003
4. V. Strouhal, "Uber eine Besondere Art der Tonerregung," Annalen der Physik und Chemie, v. V, pp. 217-251
5. Horace Lamb, *Hydrodynamics*, Sixth Edition, Section 68, Dover Publications, 1945
6. Stephen P. Timoshenko and James M. Gere, *Theory of Elastic Stability*, Second Edition, Section 1.2, McGraw-Hill Book Company, New York
7. W. D. Iwan and R. D. Blevins, "A Model for Vortex-Induced Oscillation of Structures," Journal of Applied Mechanics, v. 41, pp. 581-586, 1974
8. O. M. Griffin and S. E. Ramberg, "Some Recent Studies of Vortex Shedding with Applications to Marine Tubulars and Risers," Journal of Energy Resources Technology, v. 104, pp. 2-13, 1982
9. T. Sarpkaya, "Vortex-Induced Oscillations," Journal of Applied Mechanics, v. 46, pp. 241-258, 1979
10. J. R. Morison, M. P. O'Brien, J. W. Johnson and S. A. Schaaf, "The Force Exerted by Surface Waves on Piles," Petroleum Transactions (American Institute of Mining Engineers), v. 189, pp. 149-154, 1950